Modeling of flow around a wind rotor HAWT Application to the dynamic stall

Ali NOUIOUA* and Rabah DIZENE
Advanced Mechanics Laboratory (AML),
University of Science and Technology Houari Boumediene (USTHB),
Algiers, ALGERIA
E-mail: nouioua19@yahoo.fr
Rabah.dizene@gmail.com

***Abstract*—The study of a horizontal axis wind turbine (HAWT) subject to operating conditions in the presence of wind is very complex, because the machine is subject to an instantaneous change in velocity and wind direction can lead inevitably turbine blades undergoing dynamic stall. The present work is a two-dimensional numerical simulation of the instantaneous variation of the wind direction relative to the turbine blade, compared to experimental data available in the literature. The effect of varying the angle of incidence of an S809 profile is studied using a URANS approach to predict the stall. The turbulence modeling is performed using the k-ε model and the k-μ SST. FLUENT software is used for the numerical solution of equations URANS. The results show the importance of taking into account the behavior of the unsteady flow analysis in order to obtain an accurate estimate of the aerodynamic loads acting on the turbine.**

Keywords-CFD; dynamic stall; wind turbine HAWT; Fluent; airfoil.

I. INTRODUCTION

The aerodynamic study is a science of studying the flow of gas (usually air) behavior around an obstacle. In other words, to study the interaction between the solid medium and the fluid medium in motion.

Unfortunately, the experimental study is expensive and it is not clear under most cases.

Predict the phenomenon of dynamic stall of a turbulent flow around a rotor blade HAWT This work aims. The profile of the blade chosen for these simulations is the NREL (National Renewable Energy Laboratory) S809. We chose this profile because there is a large number of an experiment in the literature about it.

The variation of the velocity field is described by a C++ program is introduced in the solver. The turbulence modeling is provided by the use of three turbulence models.

In order to validate this approach a numerical comparison of numerical results with experimental data [1] [2] following the literature was made. The flow is considered around the animated 2D profile of an oscillating movement, simulated by a field of variable-speed impact.

II. MATHEMATICAL MODEL

For an incompressible flow, the equations governing the conservation of mass and momentum are (averaged by the procedure of Reynolds) respectively given by:

Equation of continuity

$$\frac{\partial U_i}{\partial x_i} = 0 \tag{1}$$

Equation of momentum

$$\frac{\partial U_i}{\partial t} + U_j \frac{\partial U_i}{\partial x_j} = -\frac{1}{\rho}\frac{\partial P}{\partial x_i} + \upsilon \frac{\partial^2 U_i}{\partial x_j \partial x_j} \tag{2}$$

Among the many models of Turbulence, The computer code Fluent has three closure methods based on the statistical approach:

- The k-ε model and its variants [3]
- The turbulence model k-ω [4]
- The Reynolds stress model (RSM) and its variants

We look at these three turbulence models, since Fluent offers other models such as Spalart-Allmaras and also the LES approach.

III. NUMERICAL MODELLING

The study of this problem involves solving a system of mathematical equations, partial derivatives of the elliptical type. This approach requires a digital channel.

We opted in this study to the use of computer code as FLUENT solver, and GAMBIT for the geometric description and the mesh.

A. Finite volume method

Several methods of discretization of differential equations in partial derivatives are used such as the finite volume method, finite differences and finite elements.

The FLUENT code uses the finite volume method, because it provides a much greater generality in its formalism, its conservative treatment as well as its adaptation to the physical problem and its simplicity in terms of linearization. These criteria are given to this method, a numerical stability and more effective convergence

B. Domain and mesh

The dimensions of the field have the following calculations: A string of 25, a length of 32.5 including 12.5 ropes upstream of the trailing edge 20 and downstream.

The number of upstream Reynolds used for these simulations is 106, the mesh is structured, this mesh is shown in Figure 1, it has 124,451 nodes.

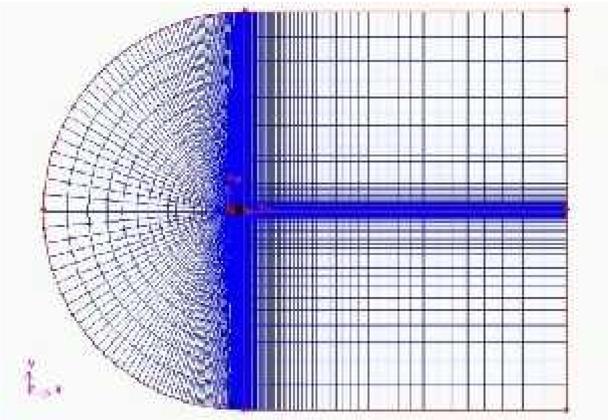

Fig. 1. Mesh field of study.

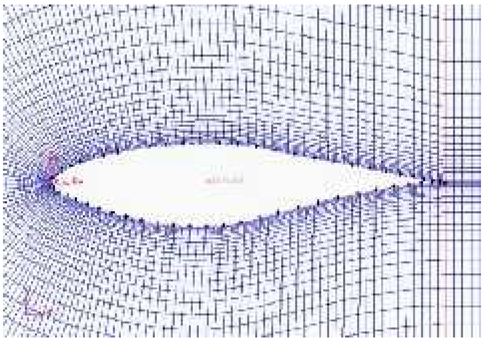

Fig. 2. Final mesh around the profile.

C. Equation of velocity field

For this very important step in our study established a program 'C + +' For What can vary the angle of incidence or the velocity versus time, the equation governing the variation of the velocity field is described as follows

$$\alpha = \alpha 0 + \alpha m \cos (\Omega t) \quad (3)$$

With: α0 the average incidence angle, αm the maximum amplitude of the oscillations and the oscillation frequency Ω.

IV. RESULTS

The results of the numerical simulation presented are obtained using the resolution of Navier-Stocks for a 2D incompressible flow with a Reynolds number Re = 10^6.

A qualitative discussion is done through the presentation of isovitesse unsteady values respectively with the standard k-ε model, RNG k-ε and k-ω SST.

The confirmation of the foregoing description is achieved through the presentation of the distribution of the pressure coefficient in the same conditions, respectively for the three turbulence models mentioned just before.

Finally ends by showing significant quantitative results regarding the lift coefficient obtained with the three models and compared with experimental results.

A. Velocity distribution

Figures 3, 4 and 5 show the average velocity of the flow around the profile for the three models, for α = 15 °.

Is observed at α = 15 ° have a flow that starts off at α = 20 ° the flow is completely off on the upper surface.

Moreover, we observe that the stall vortex arises just behind the leading edge as shown in the model k-ε RNG and k-ω SST.

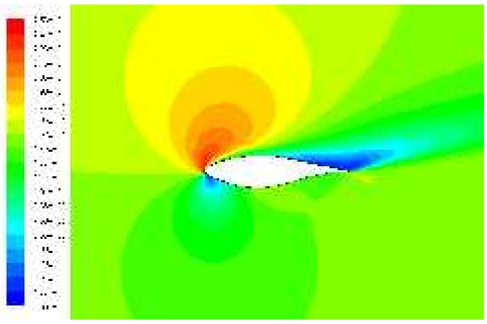

Fig. 3. Isovaleurs speed (STANDARD k-ε).

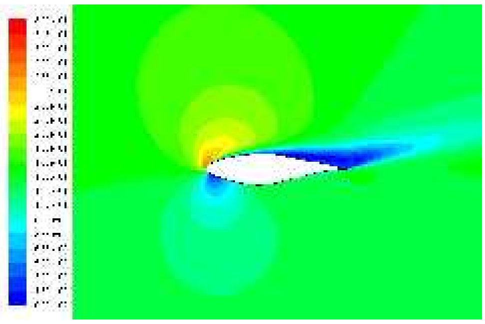

Fig. 4. Isovaleurs speed (RNG k-ε).

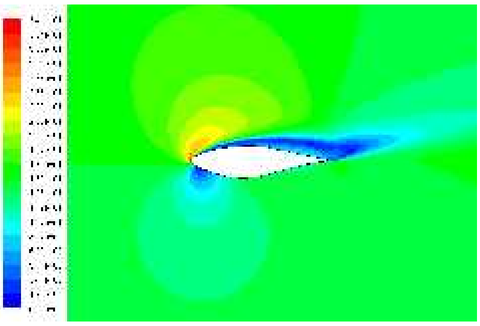

Fig. 5. Isovaleurs speed (k-ω SST).

B. Distribution of the static pressure

Figures 6, 7 and 8 show the distributions of the static pressure as a function of the position x / c for the three models for an angle of attack of α = 15°,

the representation of the pressure and substantially similar between the three patterns on the entire surface of the profile.

We respect the existence of a bull that is peeling around (x / c = 0, 45), which is consistent with results found in the literature (Reuss Ramsay, M 1995). [5]

For different angles notable on these distributions between the three models, however, we note the strong negative pressure α = 15 ° and are increasing in α = 20 ° to the upper surface of the profile. This negative pressure peak located just after the leading edge, and decreases as the flow moves towards the trailing edge.

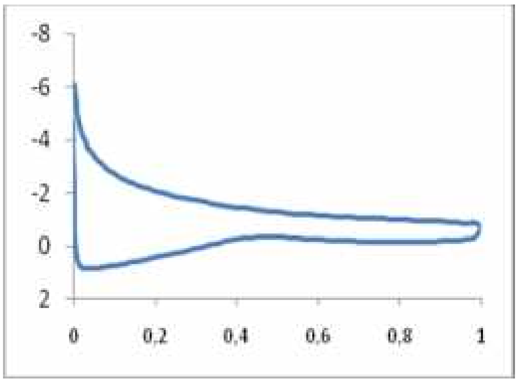

Fig. 6. Pressure coefficients depending on the position x/c (k ε-STANDARD).

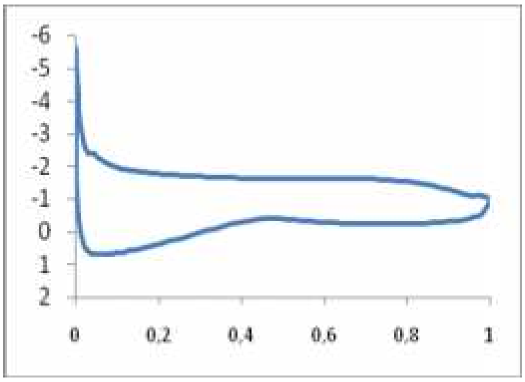

Fig. 7. Pressure coefficients depending on the position x/c (RNG k-ε).

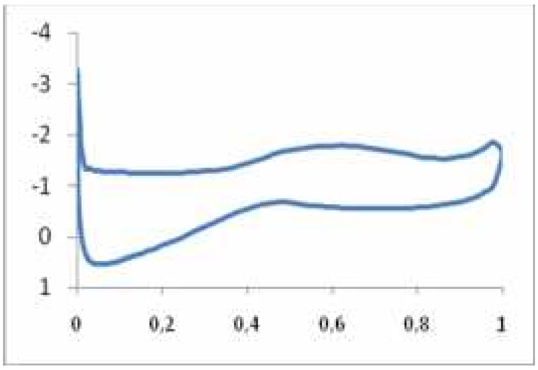

Fig. 8. Pressure coefficients depending on the position x/c (k-ω SST).

The comparison of the phenomenon among the three turbulence models shows that the model k-ε standard differs from the other two dice value α = 25 ° where the distributions obtained remain relatively constant pressure on the surface of the upper surface and towards the leading edge.

C. Lift coefficient

The prediction of the flow in all its complexity is important not only to determine the average power recovered but also to anticipate cyclical efforts that induce material fatigue.

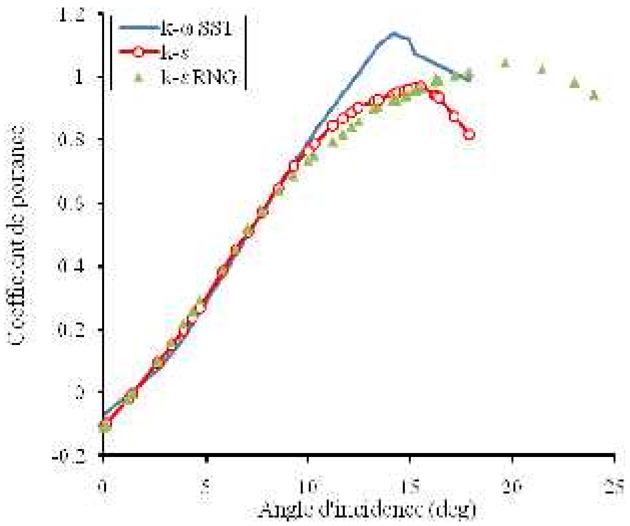

Fig. 9. Lift coefficients for the three turbulence models for Re = 10^6.

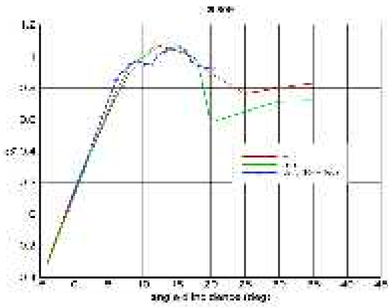

(a)

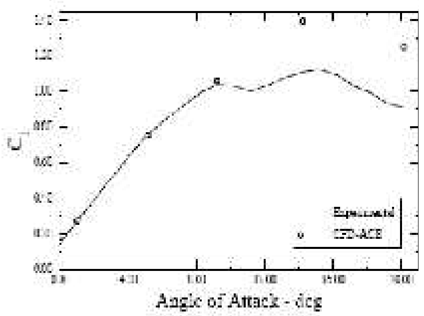

(b)

Fig. 10. Experimental results of the lift coefficient as a function of the angle of attack according (a) I.Dobrev [1] and (b) P.Walter [2]

Figure 9 shows the evolution of the lift coefficient as a function of the angle of incidence α during a time interval T = 2.75 sec and a Reynolds 10^6.

The maximum values of Cl are predicted in the range of angles of attack of α=15° α=22°, whereas the experimental shows a Cl Precipitation is between α = 10° α = 18 °.

However, the values of this calculation are above the calculated and measured values in reference [1] [2]. The results of k-ε standard and k-ε RNG are less precise than those of k-ω SST [1], compares the experimental values.

V. Conclusion

A Modelling of a field of variable speed is proposed in this study to simulate the changes in wind speed which is subjected to a horizontal axis wind turbine rotor (HAWT) profile NREL S809.

The results of unsteady and turbulent calculations are based on the discussion of the velocity fields, static pressure and the evolution of the lift coefficient.

The results of calculation of the overall evolution of the flow field around the profile show the same behavior as a whole the results found in the literature [5], which show the onset of stall from the leading edge and α = 15 °.

The results of static pressure coefficients breed so satisfying transition area suspected to be located at a distance of 40% chord from the leading edge, which is also the headquarters of the early separation of the layer.

However, the experimental curves show perturbations of the boundary layer dice position x = 20% of rope.

The lift coefficients Cl our calculations show a very satisfactory prediction, compared to the experience [2] since the stall is suspected to be approximately α = 20 °. Compared with the experiment, the k-modelsω SST and RSM seem best suited for the simulation of the dropout phenomenon.

Further work on the effects of variation of the angle of attack is taken as opportunities to present this work because there are several mechanisms to master using other models which are empirical or periodicals.

REFERENCES

[1] Ivan DOBREV hybrid active surface for analysis of the aerodynamic behavior of a wind rotor blades rigid or deformable.
[2] Walter P. Wolfe, Stuart S. Ochs (1997) Engineering Sciences Center Sandia National Laboratories Albuquerque CFD Calculations of S809 Aerodynamic Characteristics.
[3] DAVID WILCOX C., "Turbulence Modeling for CFD", DCW Industries, Inc., The Cafiada, California 91011, November 1994.
[4] ARNE JOHANSSON, "Engineering Turbulence Models and Their Development, With Emphasis on Explicit Algebraic Reynolds Stress Models.
[5] R. R. RamsayJ. Mr. JaniszewskaG.M. Gregorek The Ohio State University Columbus, Ohio Wind Tunnel Testing of Three S809 Spoiler Configurations for use on Horizontal Axis Wind Turbines.
[6] Sorensen, NN (Riso), Michelsen, JA (TU-Dk), and Schreck, S. (NREL) 'Navier-Stokes predictions of the NREL Phase-IV rotor in the NASA Ames 80-by-120 wind tunnel.
[7] R.DIZENE, A.NOUIOUA and L.BOURANE (USTHB) 2010 'Modelling of a flow around a wind turbine blade, Velocity fields oscillating'